Available online at www.sciencedirect.com
SCIENCE DIRECT®
Journal of Computational and Applied Mathematics 192 (2006) 339–352
JOURNAL OF COMPUTATIONAL AND APPLIED MATHEMATICS
www.elsevier.com/locate/cam

Finite element method solution of electrically driven magnetohydrodynamic flow☆

A.I. Nesliturk[a,*], M. Tezer-Sezgin[b]

[a] *Department of Mathematics, Izmir Institute of Technology, 35430 Izmir, Turkey*
[b] *Department of Mathematics, Middle East Technical University, 06531 Ankara, Turkey*

Received 27 January 2005; received in revised form 20 May 2005

Abstract

The magnetohydrodynamic (MHD) flow in a rectangular duct is investigated for the case when the flow is driven by the current produced by electrodes, placed one in each of the walls of the duct where the applied magnetic field is perpendicular. The flow is steady, laminar and the fluid is incompressible, viscous and electrically conducting. A stabilized finite element with the residual-free bubble (RFB) functions is used for solving the governing equations. The finite element method employing the RFB functions is capable of resolving high gradients near the layer regions without refining the mesh. Thus, it is possible to obtain solutions consistent with the physical configuration of the problem even for high values of the Hartmann number. Before employing the bubble functions in the global problem, we have to find them inside each element by means of a local problem. This is achieved by approximating the bubble functions by a nonstandard finite element method based on the local problem. Equivelocity and current lines are drawn to show the well-known behaviours of the MHD flow. Those are the boundary layer formation close to the insulated walls for increasing values of the Hartmann number and the layers emanating from the endpoints of the electrodes. The changes in direction and intensity with respect to the values of wall inductance are also depicted in terms of level curves for both the velocity and the induced magnetic field.

Keywords: MHD flow; FEM; Residual-free bubble functions

☆ Supported by TUBITAK-Scientific and Technical Research Council of Turkey.
* Corresponding author. Tel.: +90 232 750 7522; fax: +90 232 750 7509.
E-mail address: alinesliturk@iyte.edu.tr (A.I. Nesliturk).

0377-0427/$ - see front matter © 2005 Elsevier B.V. All rights reserved.
doi:10.1016/j.cam.2005.05.015

1. Introduction

The problem of the flow of incompressible, viscous, electrically conducting fluids in channels with partly conducting and partly nonconducting walls under a uniform transverse magnetic field has many practical applications in the field of magnetohydrodynamic (MHD). Several numerical methods such as FDM [14,15], FEM [16,17,19,4], BEM [18] produced physical numerical results in several configuration of interest but Hartmann number M could not be increased more than 100. In our recent work [10], the Galerkin finite element method with standard piecewise linear polynomials enriched by the residual-free bubble (RFB) functions is used to solve MHD flow problem in channels with partly insulated and partly conducting walls under oblique magnetic field. The RFB method was first proposed by Brezzi and Russo in [3] for the advection-diffusion equation and the stability of the method has been investigated for a wide range of critical Peclet number [11,1,6,12,2,7]. The RFB functions in the framework of the standard Galerkin FEM enable us to resolve layers without refining the mesh and we are able to compute accurate numerical approximations to the solution of the MHD problem for the range of Hartmann number $10^2 < M < 10^6$ in a number of benchmark problems [10]. Before employing the bubble functions in the global problem, we have to find them inside each element by means of a local problem. This can be achieved by approximating the bubble functions by a nonstandard finite element method based on the local problem and then using these approximations in place of exact bubble functions in the global problem.

The present paper is an application of the technique mentioned above to the MHD flow in a duct where the flow is driven down by the electrodes placed in the middle of the walls which are perpendicular to the applied magnetic field. The walls parallel to the applied magnetic field are kept at constant inductance but opposite in sign. On the insulated parts of the walls in which the electrodes are placed, the same magnetic field values are continued from the parallel walls. There is no need for the pressure gradient to drive the fluid down the duct. This is achieved by the electrodes connected to the external circuits. The external magnetic field causes the appearance within the fluid of an induced current which can be made to flow in these external circuits. In this manner, some of the internal energy of the fluid is given up to the exterior as utilizable electrical energy, especially for high Hartmann numbers. Large values of Hartmann number means more electrical energy produced out of this MHD channel which is the basic idea of MHD power generators. These are some of the reasons for the problem to be of considerable theoretical and physical importance. The problem itself, treating an electrically driven MHD flow in a rectangular duct subject to mixed boundary conditions on the same wall, retains its importance to obtain the solution for high Hartmann numbers.

2. Governing equations

The basic equations governing the flow have been obtained by Dragoş [5], the only difference being that the pressure gradient $\mathrm{d}p/\mathrm{d}z = 0$. These are, in nondimensional form, as follows:

$$\left.\begin{aligned} \nabla^2 V + M\frac{\partial B}{\partial y} &= 0 \\ \nabla^2 B + M\frac{\partial V}{\partial y} &= 0 \end{aligned}\right\} \quad \text{in } \Omega, \tag{1}$$

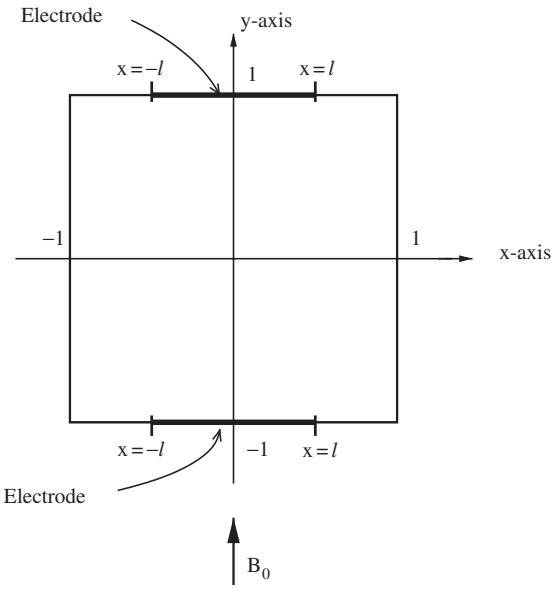

Fig. 1. Problem statement.

where Ω denotes the section of the duct (see Fig. 1). $V(x, y)$ and $B(x, y)$ are the velocity and the induced magnetic field variables in the z-direction, respectively. $M = B_0^2 a^2 \sigma/\zeta$ is the Hartmann number where B_0 is the intensity of the applied magnetic field, a is the characteristic length of the duct, σ and ζ are the electrical conductivity and the coefficient of viscosity of the fluid, respectively. The boundary conditions are

$$\begin{aligned}
&V = 0, \quad y = \mp 1 \quad \text{and} \quad x = \mp 1,\\
&B = k, \quad x > l, \quad y = \mp 1 \quad \text{and} \quad x = +1,\\
&B = -k, \quad x < -l, \quad y = \mp 1 \quad \text{and} \quad x = -1,\\
&\frac{\partial B}{\partial y} = 0, \quad -l \leqslant x \leqslant l, \quad y = \mp 1,
\end{aligned} \tag{2}$$

where k is a constant ($k \leqslant 1$). The velocity is zero everywhere on the walls. The normal derivative of the induced magnetic field is zero on the electrodes, the conducting portions of the walls $y = \mp 1$. On the other parts of the boundary, the induced magnetic field takes a constant value k but opposite in sign when $x = +l$, $x > l$ with $y = \mp 1$ and $x = -l$, $x < -l$ with $y = \mp 1$.

Before we go further, we remark that we use standard notation for function spaces: $L^2(\Omega)$ is the space of square-integrable functions in Ω, $H^1(\Omega)$ is the Sobolev space of $L^2(\Omega)$ functions whose derivatives are square-integrable in Ω and $H_0^1(\Omega)$ is the Sobolev space of $H^1(\Omega)$ functions in Ω with zero value on the boundary $\partial\Omega$. Also $(\cdot, \cdot)$ denotes the L_2 inner product on Ω.

3. Finite element formulation

Let Γ_1 be the part of the boundary where Dirichlet boundary conditions are imposed for the magnetic field variable B. Let $\mathscr{V}_0 = H_0^1(\Omega)$ and $\mathscr{B} = \{B | B \in H^1(\Omega),\ B|_{\Gamma_1} = q\}$ where q is a constant and equal to $-k$ or $+k$ depending on the part of the boundary (see boundary conditions at (2)). Further let $\mathscr{B}_0$ be the counterpart of $\mathscr{B}$ in which q vanishes on Γ_1. The problem (1) with boundary conditions (2) can be equivalently stated as the following variational problem: find $V \in \mathscr{V}_0$ and $B \in \mathscr{B}$ such that

$$c(V, B; \tilde{V}, \tilde{B}) = 0 \quad \text{for all } (\tilde{V}, \tilde{B}) \in \mathscr{V}_0 \times \mathscr{B}_0, \tag{3}$$

where

$$c(V, B; \tilde{V}, \tilde{B}) = -(\nabla V, \nabla \tilde{V}) + (M B_{,y}, \tilde{V}) - (\nabla B, \nabla \tilde{B}) + (M V_{,y}, \tilde{B}).$$

To specify Galerkin finite element method we choose a partition $\mathscr{K}$ of Ω consisting of bilinear quadrilateral elements in the standard way (e.g., no overlapping, no vertex on the edge of neighbouring element). Let $\mathscr{V}_{h0} \times \mathscr{B}_h$ denote the finite dimensional subspace of $\mathscr{V}_0 \times \mathscr{B}$. The finite dimensional subspaces that we wish to work are given by

$$\mathscr{V}_{h0} = \mathscr{V}_{10} + \mathscr{V}_b = \mathscr{V}_1 \oplus \left(\bigcup_K \mathscr{B}_V(K) \right) \subset \mathscr{V}_0 = H_0^1(\Omega),$$

$$\mathscr{B}_h = \mathscr{B}_1 + \mathscr{B}_b = \mathscr{B}_1 \oplus \left(\bigcup_K \mathscr{B}_M(K) \right) \subset \mathscr{B} = H^1(\Omega),$$

where $\mathscr{V}_{10}$ and $\mathscr{B}_1$ denote the finite element spaces of continuous, piecewise bilinear polynomials defined over quadrilateral elements, $\mathscr{B}_V(K) \subset H_0^1(K)$ and $\mathscr{B}_M(K) \subset H_0^1(K)$. Moreover the finite dimensional spaces $\bigcup_K \mathscr{B}_V(K)$ and $\bigcup_K \mathscr{B}_M(K)$ are spanned by the so-called RFB functions which will be specified later. We assume that if $\overline{B}_h \in \mathscr{B}_h$ then $\overline{B}_h$ satisfies the Dirichlet boundary conditions in (2) on the corresponding part of the boundary and that $\mathscr{B}_{h0}$ and $\mathscr{B}_{10}$ are the counterparts of $\mathscr{B}_h$ and $\mathscr{B}_1$, respectively, with the vanishing Dirichlet boundary condition on Γ_1. That is, if $\overline{B}_h \in \mathscr{B}_h$ then $\overline{B}_h = B_h + q_1$ where $B_h \in \mathscr{B}_{h0}$ and q_1 is the given bilinear function that satisfy the Dirichlet boundary conditions on Γ_1 and zero at degrees of freedom.

Let us state the standard Galerkin finite element method for the problem (3) with our choice of finite dimensional spaces: Find $V_h \in \mathscr{V}_{h0}$ and $B_h \in \mathscr{B}_{h0}$ such that

$$c_h(V_h, B_h; \tilde{V}_h, \tilde{B}_h) = -c_h(0, q_1; \tilde{V}_h, \tilde{B}_h) \quad \text{for all } (\tilde{V}_h, \tilde{B}_h) \in \mathscr{V}_{h0} \times \mathscr{B}_{h0}, \tag{4}$$

where

$$c_h(V_h, B_h; \tilde{V}_h, \tilde{B}_h) = -(\nabla V_h, \nabla \tilde{V}_h) + (M B_{h,y}, \tilde{V}_h) - (\nabla B_h, \nabla \tilde{B}_h) + (M V_{h,y}, \tilde{B}_h).$$

Bubble functions are required to vanish on the boundary ∂K of each element K by definition. For the particular case of the RFBs, we define the bubble component V_b of V_h and B_b of B_h by also requiring that the pair $\{V_h, B_h\}$ satisfy the following differential equation (1) in the interior of each K and zero

elsewhere. That is,

$$\begin{aligned}
&\nabla^2(V_1 + V_b) + M(B_1 + B_b + q_1)_{,y} = 0 \quad \text{in } K,\\
&\nabla^2(B_1 + B_b + q_1) + M(V_1 + V_b)_{,y} = 0 \quad \text{in } K,\\
&V_b = B_b = 0 \quad \text{on } \partial K.
\end{aligned} \tag{5}$$

or equivalently,

$$\begin{aligned}
&\nabla^2 V_b + MB_{b,y} = -MB_{1,y} - Mq_{1,y} - \nabla^2 V_1 \quad \text{in } K,\\
&\nabla^2 B_b + MV_{b,y} = -MV_{1,y} - \nabla^2 B_1 - \nabla^2 q_1 \quad \text{in } K,\\
&V_b = B_b = 0 \quad \text{on } \partial K.
\end{aligned} \tag{6}$$

In (4), take $\tilde{V}_h = \tilde{V}_b$ and $\tilde{B}_h = \tilde{B}_b$ on K and $\tilde{V}_h = \tilde{B}_h = 0$ elsewhere to obtain

$$c_h(V_h, B_h + q_1; \tilde{V}_b, \tilde{B}_b)_K = 0. \tag{7}$$

Obviously the subscript K indicates that integration is restricted to the element K. Our choice of the RFBs in Eq. (5) ensures that the Eq. (7) is satisfied automatically. Then the numerical method that we implement is obtained by setting $\tilde{V}_h = \tilde{V}_1$ and $\tilde{B}_h = \tilde{B}_1$ in Eq. (4): find $V_h = V_1 + V_b \in \mathscr{V}_{h0}$ and $B_h = B_1 + B_b \in \mathscr{B}_{h0}$ such that

$$c_h(V_1, B_1; \tilde{V}_1, \tilde{B}_1) + c_h(V_b, B_b; \tilde{V}_1, \tilde{B}_1) = -c_h(0, q_1; \tilde{V}_1, \tilde{B}_1) \quad \text{for all } (\tilde{V}_1, \tilde{B}_1) \in \mathscr{V}_{10} \times \mathscr{B}_{10}, \tag{8}$$

where

$$\begin{aligned}
c_h(V_1, B_1; \tilde{V}_1, \tilde{B}_1) &= -(\nabla V_1, \nabla \tilde{V}_1) + (MB_{1,y}, \tilde{V}_1) - (\nabla B_1, \nabla \tilde{B}_1) + (MV_{1,y}, \tilde{B}_1),\\
c_h(V_b, B_b; \tilde{V}_1, \tilde{B}_1) &= -(\nabla V_b, \nabla \tilde{V}_1) + (MB_{b,y}, \tilde{V}_1) - (\nabla B_b, \nabla \tilde{B}_1) + (MV_{b,y}, \tilde{B}_1),\\
c_h(0, q_1; \tilde{V}_1, \tilde{B}_1) &= +(Mq_{1,y}, \tilde{V}_1) - (\nabla q_1, \nabla \tilde{B}_1),
\end{aligned}$$

where bubble functions $\{V_b, B_b\}$ are defined in terms of $\{V_1, B_1, q_1\}$ by Eq. (6). Thus the enrichment of the finite element spaces of piecewise bilinear functions by bubble functions can be viewed as a modification of the Galerkin formulation by the addition of four additional terms, from which the terms $(MB_{b,y}, \tilde{V}_1)$ and $(MV_{b,y}, \tilde{B}_1)$ are actually responsible for the stability of the numerical method (see [10]).

4. Computation of bubble functions

Before employing the numerical method (8), we have to find the RFB part $\{V_b, B_b\}$ of the numerical solution $\{V_h, B_h\}$ by means of the local problem (6) and assemble the contribution coming from the bubble part of the solution to the global formulation (8). This can be done by a two-level finite element method (TLFEM) [6]. In this method we decompose the approximations for velocity and the magnetic

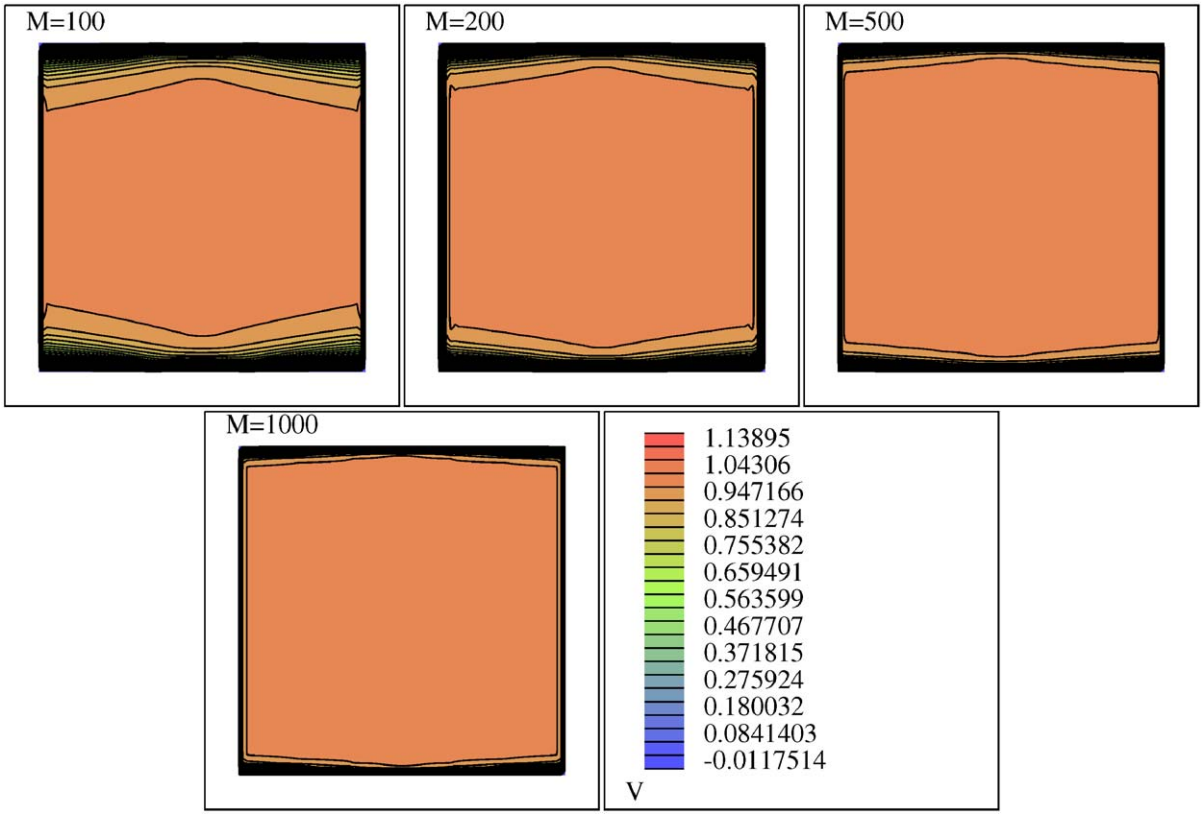

Fig. 2. Velocity field for different Hartmann numbers M: $k = 1$, $l = 0.3$.

field into their basis functions and solve the resulting local equations by a nonstandard finite element method inside each element. Application of the TLFEM to the problem under consideration is as follows.

Consider the system of equations in (6). Vanishing property of the bubble functions on element boundaries enables us to decouple this system of equations. The change of variable

$$\begin{aligned} U_b &= V_b + B_b, \\ W_b &= V_b - B_b \end{aligned} \tag{9}$$

transforms the equations in (6) into a pair of the convection-diffusion problems:

$$\begin{aligned} &\nabla^2 U_b + M U_{b,y} = -(\nabla^2 V_1 + M V_{1,y}) - (\nabla^2 B_1 + M B_{1,y}) - (\nabla^2 q_1 + M q_{1,y}) \quad \text{in } K, \\ &\nabla^2 W_b - M W_{b,y} = -(\nabla^2 V_1 - M V_{1,y}) + (\nabla^2 B_1 - M B_{1,y}) + (\nabla^2 q_1 - M q_{1,y}) \quad \text{in } K, \\ &U_b = W_b = 0 \quad \text{on } \partial K. \end{aligned} \tag{10}$$

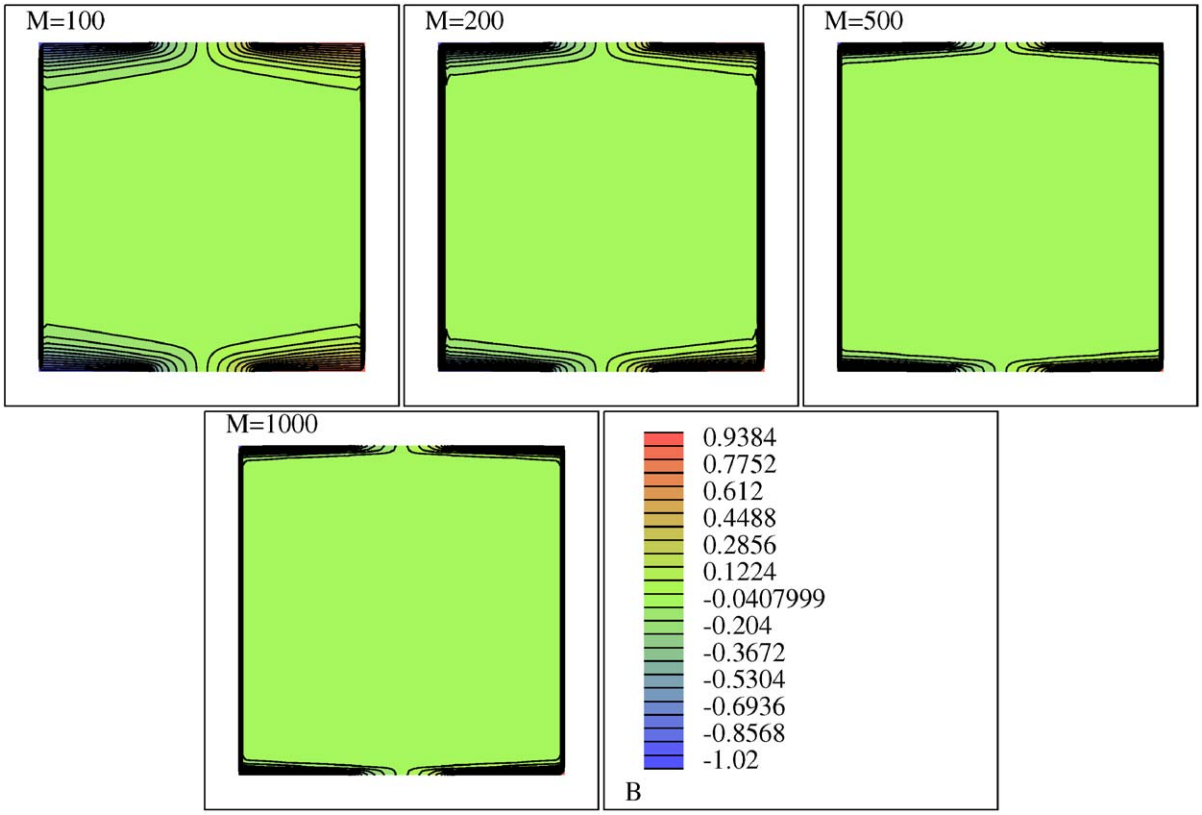

Fig. 3. Magnetic field for different Hartmann numbers M: $k = 1$, $l = 0.3$.

Let us write $\{V_1, B_1\}$, the polynomial parts of the approximation, in terms of bilinear basis functions:

$$V_1 = \sum_{i=1}^{nen_V} V_i \psi_i,$$

$$B_1 = \sum_{i=1}^{nen_B} B_i \psi_i, \tag{11}$$

where nen_V is the number of degrees of freedom for the velocity, nen_B is the number of degrees of freedom for the magnetic field, V_i is the nodal approximation value for the velocity variable and B_i is the nodal approximation value for the magnetic field variable. Now it is appropriate to decompose new

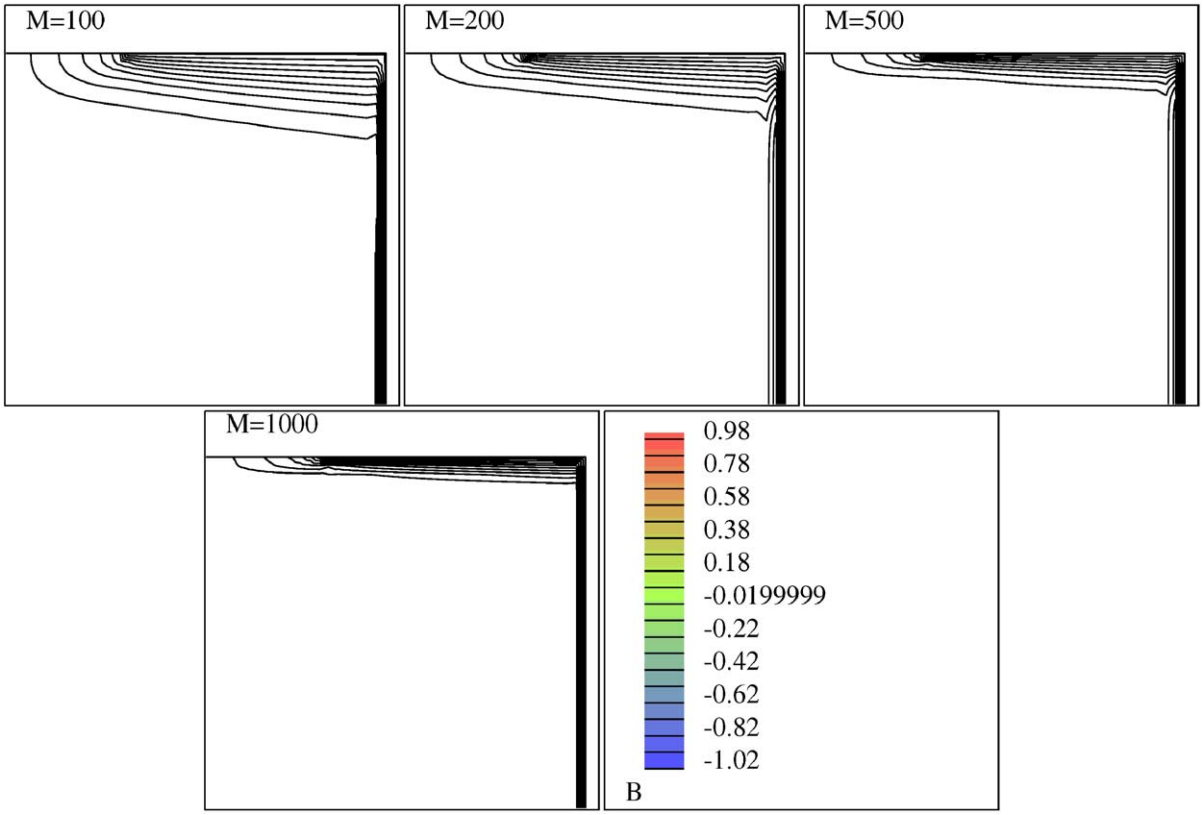

Fig. 4. Magnetic field in the first quadrant ($0 \leqslant x \leqslant 1,\ 0 \leqslant y \leqslant 1$): $k = 1, l = 0.3$.

variables U_b and W_b as follows:

$$U_b = U_b^V + U_b^B + U_b^q = \sum_{i=1}^{nen_V} V_i \varphi_i^V + \sum_{i=1}^{nen_B} B_i \varphi_i^B + \varphi^q,$$

$$W_b = W_b^V + W_b^B + W_b^q = \sum_{i=1}^{nen_V} V_i \hat{\varphi}_i^V + \sum_{i=1}^{nen_B} B_i \hat{\varphi}_i^B + \hat{\varphi}^q, \tag{12}$$

where the functions φ_i^V, φ_i^B, φ^q, $\hat{\varphi}_i^V$, $\hat{\varphi}_i^B$, $\hat{\varphi}^q$ are the bubble basis functions defined in terms of bilinear shape functions ψ_i's:

$$\nabla^2 \varphi_i^V + M \varphi_{i,y}^V = -\nabla \psi_i - M \psi_{i,y} \quad \text{in } K,$$

$$\varphi_i^V = 0 \quad \text{on } \partial K, \tag{13}$$

$$\nabla^2 \varphi_i^B + M \varphi_{i,y}^B = -\nabla \psi_i - M \psi_{i,y} \quad \text{in } K,$$

$$\varphi_i^B = 0 \quad \text{on } \partial K, \tag{14}$$

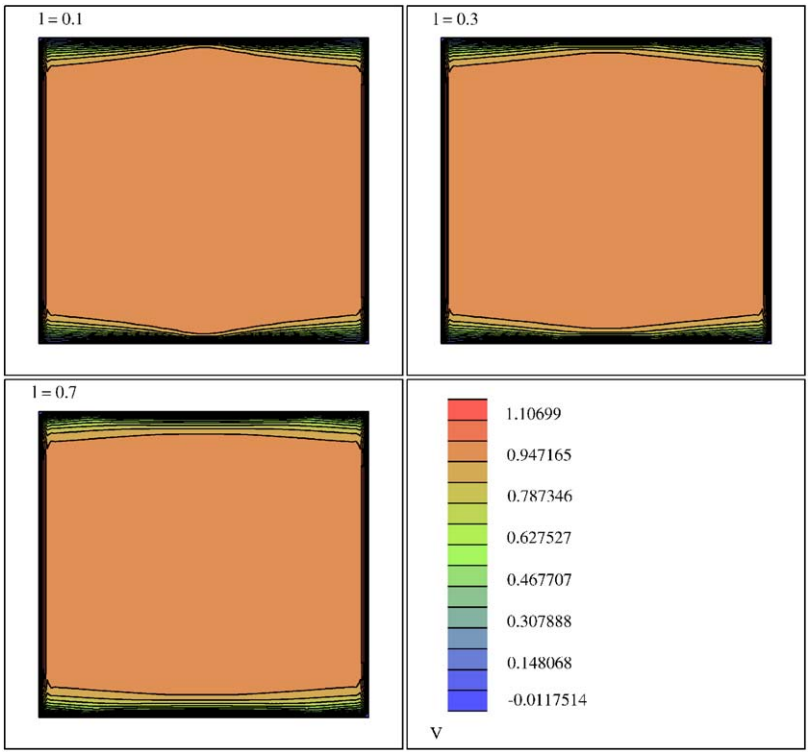

Fig. 5. Velocity field for different electrode lengths l: $M = 200$, $k = 1$.

$$\nabla^2 \varphi_i^q + M\varphi_{i,y}^q = -\nabla q_1 - M\, q_{1,y} \quad \text{in } K,$$
$$\varphi_i^q = 0 \quad \text{on } \partial K, \tag{15}$$

$$\nabla^2 \hat{\varphi}_i^V + M\hat{\varphi}_{i,y}^V = -\nabla \psi_i + M\, \psi_{i,y} \quad \text{in } K,$$
$$\hat{\varphi}_i^V = 0 \quad \text{on } \partial K, \tag{16}$$

$$\nabla^2 \hat{\varphi}_i^B + M\hat{\varphi}_{i,y}^B = \nabla \psi_i - M\, \psi_{i,y} \quad \text{in } K,$$
$$\hat{\varphi}_i^B = 0 \quad \text{on } \partial K, \tag{17}$$

$$\nabla^2 \hat{\varphi}_i^q + M\hat{\varphi}_{i,y}^q = \nabla q_1 - M\, q_{1,y} \quad \text{in } K,$$
$$\hat{\varphi}_i^q = 0 \quad \text{on } \partial K, \tag{18}$$

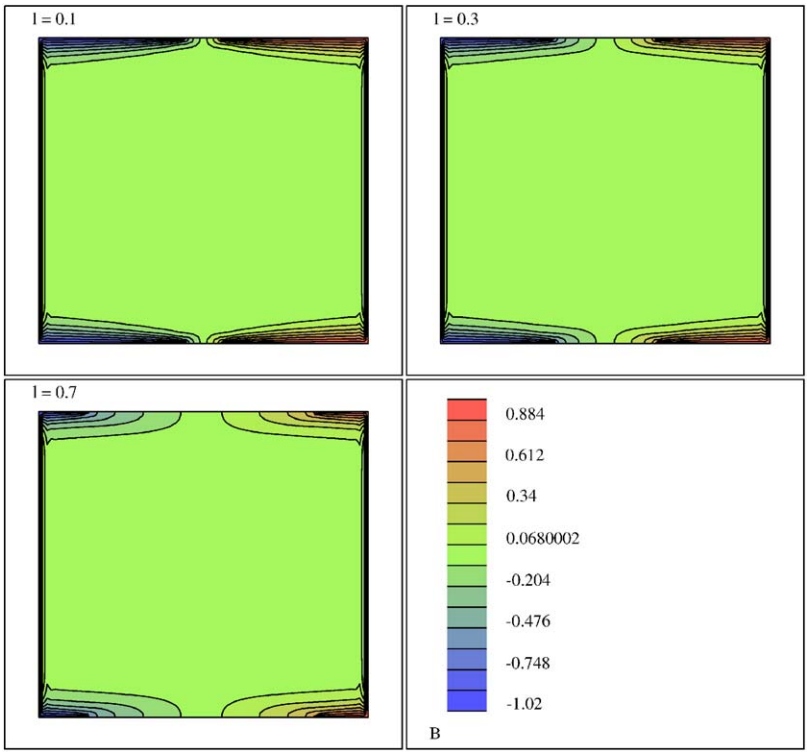

Fig. 6. Magnetic field for different electrode lengths l: $M = 200$, $k = 1$.

where i runs from 1 to nen_V for φ's and from 1 to nen_B for $\hat{\varphi}$'s. Thus the bubble components $\{V_b, B_b\}$ of the approximation can be represented in terms of bubble basis function by means of (9) and (11):

$$V_b = \frac{1}{2}\left[\sum_{i=1}^{nen_V} V_i(\varphi_i^V + \hat{\varphi}_i^V) + \sum_{i=1}^{nen_B} B_i(\varphi_i^B + \hat{\varphi}_i^B) + \varphi^q + \hat{\varphi}^q\right],$$

$$B_b = \frac{1}{2}\left[\sum_{i=1}^{nen_V} V_i(\varphi_i^V - \hat{\varphi}_i^V) + \sum_{i=1}^{nen_B} B_i(\varphi_i^B - \hat{\varphi}_i^B) + \varphi^q - \hat{\varphi}^q\right]. \tag{19}$$

Once the set of equations (13)–(18) are solved, we plug the expressions (19) into the global formulation in (8) and then solve the global problem. However, the solution of this set of equations may be difficult as much as the original problem (1). Therefore we set another layer of mesh, called submesh, inside each element and use a nonstandard finite element method on the submesh to approximate each exact bubble basis functions defined in (13)–(18). Then we use these approximations in place of φ_i^V, φ_i^B, φ^q, $\hat{\varphi}_i^V$, $\hat{\varphi}_i^B$, $\hat{\varphi}^q$ in the global formulation (8). We remark that we choose a submesh which consist of 4 by 4 or 8 by 8 bilinear rectangular elements depending on the Hartmann number and employ the Galerkin-least squares method-GLS [8] to find each approximate bubble basis functions on the submesh.

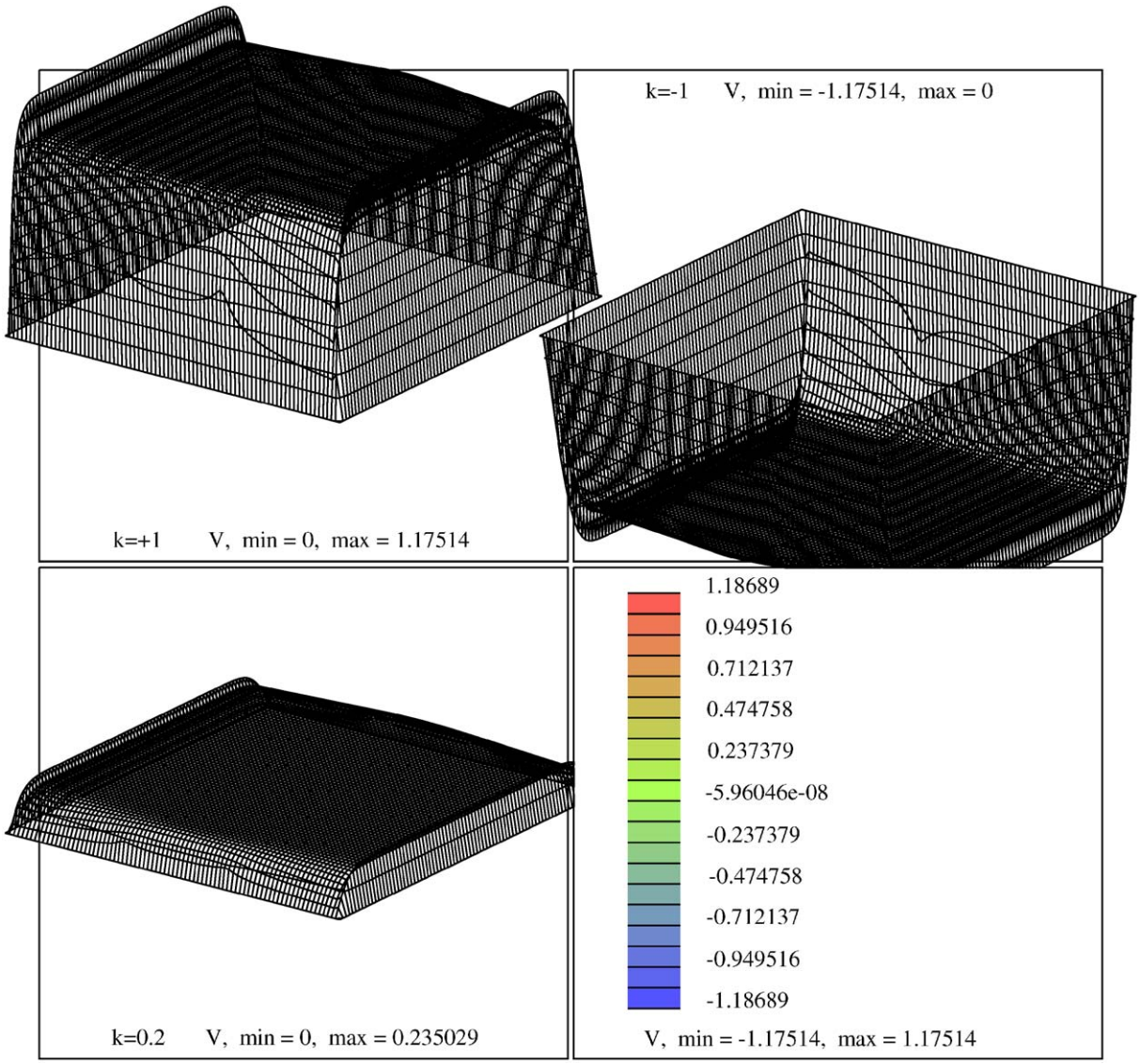

Fig. 7. Velocity field at different wall inductance: $k = 1$, $k = -1$ and $k = 0.2$, respectively ($M = 200$, $l = 0.3$).

5. Numerical results

In this section we present the details and the results of our computer implementation of the numerical method displayed in the previous sections. We have taken a long channel (duct) of square cross-section defined by

$$\{(x, y) : -1 \leqslant x \leqslant 1 \text{ and } -1 \leqslant y \leqslant 1\}.$$

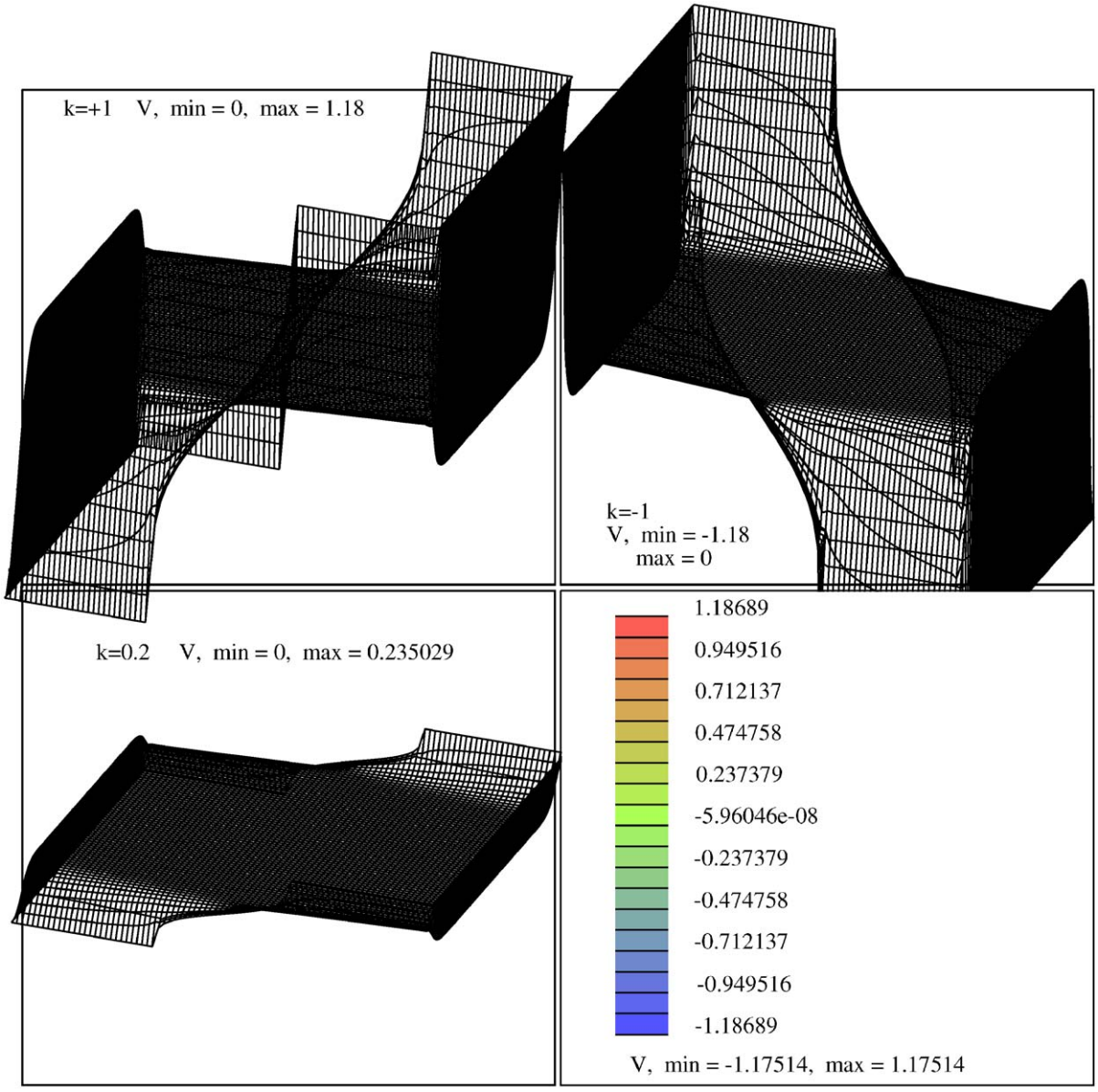

Fig. 8. Magnetic field at different wall inductance: $k = 1$, $k = -1$ and $k = 0.2$, respectively ($M = 200$, $l = 0.3$).

(see Fig. 1). This section is discretized with a uniform 80×80 mesh of bilinear (four node) quadrilateral elements. Computations are carried out for several values of the wall inductance k, the Hartmann number M and the electrode length l to indicate the effect of these parameters on the behaviours of the velocity and the induced magnetic field of the flow. We remark that only the linear parts of the approximation are used in visualizations.

Figs. 2 and 3 display equivelocity and current (induced magnetic field) contours, respectively, for the wall inductance $k = 1$ and the electrode length $l = 0.3$ at several values of the Hartmann number. It can be observed, from these figures, that boundary layer formation makes a strong appearance for both the velocity and the magnetic field for large values of M. As the Hartmann number increases, the velocity of the flow becomes more uniform throughout the region except a very narrow part of the domain confined to the vicinity of the walls. For the induced magnetic field, we have a layer formation, emanating from the points of discontinuity $(\mp l, \mp 1)$ on the boundary. The structure of these layers shows similarity to the solution of the MHD flow on the half plane $y > 0$ with a conducting portion [13,9]. There, the layers propagating from the endpoints of the conducting part of the boundary is of parabolic type and have thickness $O(1/\sqrt{M})$. The layers near the insulated parallel walls are more pronounced because they are of order $O(1/M)$ [5]. Two types of boundary layers can be distinguished clearly in Fig. 4. However, as M is increased, these two set of layers are connected as a thin layer near the walls. Finally we remark that the current lines, in Fig. 3, are positive on the right half of the channel since $B = k$ $(k > 0)$ on $x = +1$ and $x > l$ with $y = \mp 1$, and negative on the left half since $B = -k$ on $x = -1$ and $x < -l$ with $y = \mp 1$.

Figs. 5 and 6 show the effect of the electrode length l on the behaviours of the velocity and the induced magnetic field, respectively. Boundary layers are less pronounced for increasing values of l for both V and B. As l is increased, the layers for the induced magnetic field, emanating from the endpoints of the electrodes, are confined to the walls $x = \mp 1$ and combined with the layers coming from the insulated parallel walls. It is apparent that the increase in value of l results in enlargement of the stagnant region, in the magnetic field, in front of the conducting portions of the boundary.

Lastly, Figs. 7 and 8 depict the behaviours of the velocity and the induced magnetic field with respect to the wall inductance k in terms of level curves for the Hartmann number $M = 200$. These level curves clearly shows that as k is increased, the values of the velocity and the induced magnetic field also increase. This indicates the importance of the initial wall inductance if we require strong intensities of the velocity and the induced magnetic field in the direction of the axis of the flow. It can also be noted that the velocity changes direction in the duct when k changes sign and the current lines change the direction in the left and the right half of the portions of the duct with respect to the sign of k. In this way, it is possible to control the direction of the flow such that connection to external circuits transfers the internal energy of the fluid to utilizable electrical energy.

References

[1] F. Brezzi, L.P. Franca, A. Russo, Further considerations on residual-free bubbles for advective-diffusive equations, Comput. Methods Appl. Mech. Engrg. 166 (1998) 25–33.

[2] F. Brezzi, T.J.R. Hughes, D. Marini, A. Russo, E. Suli, A priori error analysis of a finite element method with residual-free bubbles for advection dominated equations, SIAM J. Numer. Anal. 36 (1999) 1933–1948.

[3] F. Brezzi, A. Russo, Choosing bubbles for advection-diffusion problems, Math. Models Methods Appl. Sci. 4 (1994) 571–587.

[4] Z. Demendy, T. Nagy, A new algorithm for solution of equations of mhd channel flows at moderate Hartmann numbers, Acta Mech. 123 (1997) 135–149.

[5] L. Dragoş, Magnetofluid Dynamics, Abacus Press, Tunbridge Wells, UK, 1975.

[6] L.P. Franca, A. Nesliturk, M. Stynes, On the stability of residual-free bubbles for convection-diffusion problems and their approximation by a two-level finite element method, Comput. Methods Appl. Mech. Engrg. 166 (1998) 35–49.

[7] L.P. Franca, L. Tobiska, Stability of the residual free bubble method for bilinear finite elements on rectangular grids, IMA J. Numer. Anal. 22 (2002) 73–87.

[8] T.J.R. Hughes, L.P. Franca, G.M. Hulbert, A new finite element formulation for computational fluid dynamics: VIII. The Galerkin-least-squares method for advective-diffusive equations, Comput. Methods Appl. Mech. Engrg. 73 (1989) 173–189.
[9] J.C.R. Hunt, J.A. Shercliff, Magnetohydrodynamics at high Hartmann number, Annu. Rev. Fluid Mech. 3 (1971) 37–62.
[10] A.I. Nesliturk, M. Tezer-Sezgin, The finite element method for MHD flow at high Hartmann numbers, Comput. Methods Appl. Mech. Engrg. 194 (2005) 1201–1224.
[11] A. Russo, Bubble stabilization of finite element methods for the linearized incompressible Navier–Stokes equations, Comput. Methods Appl. Mech. Engrg. 132 (1996) 335–343.
[12] G. Sangalli, Global and local error analysis for the residual-free bubbles method applied to advection-dominated problems, SIAM J. Numer. Anal. 38 (2000) 1496–1522.
[13] M. Sezgin, Magnetohydrodynamic flow on a half-plane, Internat. J. Numer. Methods Fluids 8 (1988) 743–758.
[14] B. Singh, J. Lal, MHD axial flow in a triangular pipe under transverse magnetic field, Indian J. Pure Appl. Math. 9 (1978) 101–115.
[15] B. Singh, J. Lal, MHD axial flow in a triangular pipe under transverse magnetic field parallel to a side of the triangle, Indian J. Tech. 17 (1979) 184–189.
[16] B. Singh, J. Lal, FEM in MHD channel flow problems, Internat. J. Numer. Methods Engrg. 18 (1982) 1104–1111.
[17] B. Singh, J. Lal, FEM for unsteady MHD flow through pipes with arbitrary wall conductivity, Internat. J. Numer. Methods Fluids 4 (1984) 291–302.
[18] M. Tezer-Sezgin, BEM solution of MHD flow in a rectangular duct, Internat. J. Numer. Methods Fluids 18 (1994) 937–952.
[19] M. Tezer-Sezgin, S. Koksal, FEM for solving MHD flow in a rectangular duct, Internat. J. Numer. Methods Engrg. 28 (1989) 445–459.